Environment International 207 (2026) 109995

Contents lists available at ScienceDirect

Environment International

journal homepage: www.elsevier.com/locate/envint

Full length article

Spatial variability in the association of ambient $PM_{2.5}$ exposure with child undernutrition in sub-Saharan Africa

Patrick Attey-Yeboah [a], Paul K. Adjorlolo [b], Justice Moses K. Aheto [b], John Molitor [c], Eric S. Coker [d], Adeladza Kofi Amegah [a,e,*]

[a] Department of Biomedical Sciences, University of Cape Coast, Cape Coast, Ghana
[b] Department of Biostatistics, School of Public Health, University of Ghana, Legon – Accra, Ghana
[c] School of Nutrition and Public Health, College of Health, Oregon State University, Corvalis, USA
[d] Department of Environmental Engineering Sciences, University of Florida, Florida, USA
[e] School of Public Health, University of Cape Coast, Cape Coast, Ghana

ARTICLE INFO

Keywords:
Ambient Particulate Matter ($PM_{2.5}$)
Child undernutrition
Spatial variability
sub-Saharan Africa

ABSTRACT

Studies have associated ambient $PM_{2.5}$ exposure with child undernutrition. However, the exposure–response relationship may vary across space. We therefore investigated spatial variability in ambient $PM_{2.5}$ – child undernutrition relationship in sub-Saharan Africa (SSA) merging several waves of Demographic and Health Survey data for 34 SSA countries for the period 1998 to 2022 with satellite-derived $PM_{2.5}$ estimates. The study included 855,395 children with complete prenatal and postnatal $PM_{2.5}$ exposure data. The prenatal and postnatal $PM_{2.5}$ exposures were estimated using a weighted average of spatially-resolved annual $PM_{2.5}$ estimates. We employed a Bayesian spatial model in R-INLA incorporating a spatially varying slope at the country level to investigate the variability in the exposure–response relationship. The model adjusted for individual- and area-level confounders whilst accounting for both structured and unstructured heterogeneity. A 10 $\mu g/m^3$ increase in prenatal and postnatal $PM_{2.5}$ exposure was associated with 11% (AOR = 1.11; 95% Credible Interval [CrI]: 1.04, 1.20) and 9% (AOR = 1.09; 95% CrI: 1.04, 1.15) increased odds of stunting in SSA, respectively. A 10 $\mu g/m^3$ increase in postnatal $PM_{2.5}$ was associated with 6% (AOR = 1.06; 95 % CrI:1.02, 1.11) increased odds of wasting in SSA. The $PM_{2.5}$ exposure–response relationship varied widely within and between SSA countries and sub-regions with the estimates consistently higher in West Africa. The findings of the study call for tailored, region-specific interventions to help address the burden of child undernutrition attributable to air pollution in the SSA region.

1. Introduction

Child undernutrition remains a major public health concern in Sub-Saharan Africa (SSA) and South Asia, with more than 180 million children under 5 reported to be malnourished in these regions in 2022 (UNICEF, WHO, & World Bank Group, 2023). The consequences of child undernutrition are severe and long-lasting including compromised immune function and associated increased susceptibility to infections, impaired early childhood neurodevelopment, low educational attainment, and increased risk of infant and child mortality (Ferreira et al., 2018; Ghosh et al., 2015; Harttgen et al., 2013; Kirolos et al., 2022; Morales et al., 2023). Studies have also linked inadequate childhood nutrition to an elevated risk of chronic non-communicable diseases including type 2 diabetes and cardiovascular conditions (Bhutta et al., 2017; Grey et al., 2021; Vassilakou, 2021; Victora et al., 2008).

Studies have identified household air pollution (HAP) as an important environmental risk factor for child undernutrition in LMIC (Adekoya et al., 2022; Deng et al., 2024; Pun et al., 2021). Ambient fine particulate matter ($PM_{2.5}$) has also been identified as an important environmental risk factor for child undernutrition (Amegbor, 2022; Amegbor et al., 2023; Bora, 2021; Clarke et al., 2022; deSouza et al., 2022; Khezri et al., 2025). In SSA, interventions for addressing child undernutrition have traditionally focused on improving child feeding practices, ensuring sanitation and hygiene practices, and addressing HAP through rolling out of clean cooking solutions (Amegah, 2020; Pun et al., 2021).

However, the studies by Amegbor and colleagues (Amegbor, 2022; Amegbor et al., 2023) have provided evidence on how early-life

* Corresponding author at: Department of Biomedical Sciences, University of Cape Coast, Cape Coast, Ghana.
E-mail address: aamegah@ucc.edu.gh (A.K. Amegah).

https://doi.org/10.1016/j.envint.2025.109995
Received 29 July 2025; Received in revised form 16 November 2025; Accepted 9 December 2025
Available online 11 December 2025

environmental exposures contribute to childhood undernutrition in SSA by employing multilevel modelling to account for spatial heterogeneity at both neighbourhood and regional scales. These studies employed random intercepts to account for variation in the outcome risk across clusters and regions, but did not explicitly model spatial autocorrelation. Their approach assumes that any geographical clustering in undernutrition is independent thereby overlooking the propensity of adjacent areas to exhibit similar outcomes due to shared environmental conditions, socio-economic factors, or infrastructure (Anselin, 2022; Pickett and Pearl, 2001). In addition, random intercepts model assumes that the relationship between exposure and outcome is constant (i.e. same slope). Clarke et al. (2022) also assessed the relationship between prenatal $PM_{2·5}$ exposure and child growth in East Africa. However, their study relied on spatially linked cluster means without also formally accounting for spatial autocorrelation or modelling possible spatially varying effects.

To address these gaps in knowledge, we employed a fully Bayesian spatial framework that integrates the Besag–York–Mollié 2 (BYM2) model (Besag et al., 1991) within the Integrated Nested Laplace Approximation (INLA) framework (Lindgren and Rue, 2015; Riebler et al., 2016) and incorporated a spatially random slope to help account for spatial autocorrelation and better investigate the spatially varying effects of $PM_{2.5}$ exposure on child undernutrition outcomes. Estimation of spatially varying effects will help better inform intervention strategies for addressing the burden of child undernutrition attributable to air pollution in SSA. The complex modelling approach will also help to explicitly model spatial autocorrelation and disentangle the contribution of local clustering from that of the independent variation across regions in the observed association to help better tailor the intervention strategies.

2. Method

The study was cross-sectional in design assembling Demographic and Health Survey (DHS) data from 34 SSA countries for the period 1998 to 2022 and merging the DHS data with satellite-derived $PM_{2.5}$ estimates.

2.1. Data sources

The DHS survey is a cross-sectional nationally representative survey conducted in 95 countries including 44 SSA countries. Thirty-four (34) SSA countries qualified for inclusion in this study during the study period. This is because they were the only countries that had spatial information on sampled Enumeration Areas (EAs) to enable $PM_{2.5}$ exposure assessment. The DHS Program uses a two-stage sampling design. In the first stage, EAs are designated as primary sample units. In the second stage, households within each EA were systematically selected with eligible women aged 15–49 years in these households interviewed, and data on their birth history and health, as well as anthropometric measurement of children born in the five years preceding the survey collected. The GPS coordinates of the sampled EAs are recorded in a geographic database and was linked to the DHS data through a unique identifier. The study sample consists of 907,535 children under five years of age from singleton pregnancies from 22,400 clusters.

Average annual estimates of $PM_{2.5}$ mass concentrations were extracted from the V5.GL.02 product of the Atmospheric Composition Analysis Group (ACAG) of Washington University, USA. This gridded raster product estimates global ground-level $PM_{2.5}$ concentrations from 1998 to 2022 by combining Aerosol Optical Depth (AOD) retrievals from multiple NASA satellite instruments (MODIS, MISR and SeaWIFS) based on their observed relative uncertainties. The combined AOD is then estimated to near-surface $PM_{2.5}$ concentrations using the spatially and temporally varying geophysical relationship between the $PM_{2.5}$ and AOD simulated by the GEOS-Chem chemical transport model (Van Donkelaar et al., 2016). The geophysical estimates are subsequently calibrated to global ground-based measurements of $PM_{2.5}$ using a Geographically Weighted Regression (GWR) (van Donkelaar et al., 2021) leveraging ground-level monitored $PM_{2.5}$ datasets compiled by WHO. This model shows strong global performance compared to ground-based observations with an annual cross-validation coefficient of determination (R^2) of 0.84 and RMSE of 8.4 $\mu g/m^3$ (van Donkelaar et al., 2021). The predicted annual surface $PM_{2.5}$ concentrations have a spatial resolution of approximately 1 km × 1 km (Hammer et al., 2023, 2020; Shen et al., 2024; Van Donkelaar et al., 2016).

2.2. Merging DHS and $PM_{2.5}$ exposure data

In merging the DHS and $PM_{2.5}$ exposure data, a buffer of 5 km was implemented for rural clusters and 2 km for urban clusters to accommodate coordinate displacement and preserve respondent anonymity. $PM_{2.5}$ concentrations were assigned to these DHS clusters by overlaying the buffered clusters geographic polygon over the gridded $PM_{2.5}$ data. Annual averaged $PM_{2.5}$ concentrations were extracted for each buffered cluster. The DHS program provides geographic coordinates for sampling clusters (i.e. enumeration areas) for some countries and waves of the survey. The difference in spatial displacement (2 km urban, 5 km rural) is due to the higher population density in urban areas and hence requiring a smaller displacement to mask location of households. In rural areas, the low population density means a larger displacement is require to adequately obscure location of more spread-out households and prevent re-identification (Burgert et al., 2013). The complete dataset integrating ambient $PM_{2.5}$ exposure levels and administrative data was combined with the DHS survey data utilizing the matching keys (DHS-CLUST and v001).

2.3. Prenatal and postnatal $PM_{2.5}$ exposure assessment

Prenatal and postnatal exposures were assigned by creating a time-weighted average of the annual $PM_{2.5}$ values for the specific months of exposure for each child. Prenatal exposure was calculated as a weighted average of monthly $PM_{2·5}$ concentrations over the nine months preceding each child's date of birth. For a child born in month $b1$ of year $b2$, the weighted prenatal exposure was calculated as follows:

$$\text{Weighted prenatal exposure} = \frac{[\text{b1} \times \text{E}_{b2}] + [(9 - \text{b1}) \times \text{E}_{b2-1}]}{9}, b1 \leq 9 \quad (1)$$

where E_y denotes the annual average $PM_{2·5}$ concentration in year y. The weights $b1$ and $9 - b1$ reflect the fraction of the gestational period falling within the birth year and the preceding year, respectively.

Postnatal exposure was calculated as a weighted average of annual $PM_{2·5}$ concentrations from the child's month of birth up to the month of the household interview. For a child born in month $b1$ of year $b2$ and surveyed in month $v006$ of year $v007$, the postanal exposure was calculated as follows:

$$\text{Weighted postnatal exposure} = \frac{[(12 - b1) \times \text{E}_{b2}] + [v006 \times \text{E}_{v007}] + \left[12 \times \sum_{y=b2+1}^{v007-1} \text{E}_y\right]}{(12 - b1) + v006 + [(v007 - b2 - 1)*12]} \quad (2)$$

E_{b2} and E_{v007} represent the annual average $PM_{2\cdot5}$ concentrations in the birth year and survey year, respectively. The summation term captures exposure for the full years between birth and survey. The denominator reflects the total number of months contributing to the exposure period. Postnatal exposure was calculated for children with at least one full month of life prior to the survey. Prenatal exposure estimation required a minimum of six months of gestation preceding birth to mitigate data gaps for children born early in 1998 but whose prenatal periods extended into 1997. For these cases, we assigned 1998 monthly averages up to three prenatal months in 1997 assuming minimal temporal variation in the monthly $PM_{2\cdot5}$ concentrations across the adjacent years. Of the total 907,535 children sampled, 855,395 had complete prenatal and postnatal exposure data.

2.4. Outcome measurement

The outcomes of interest were stunting, wasting, underweight, and anaemia. Based on the 2006 WHO child growth standards, children were classified as stunted if their height-for-age z-score was below −2 standard deviations (SD) from the median of the reference population. Children were classified as wasted if their weight-for-height z-scores were below −2SD from the median of the reference population. Children were classified as underweight if their weight for age z-score was below −2SD from the median of the reference population. The DHS survey collected anthropometric data comprising height and weight measurements for children aged 0–59 months in the sampled households and was used to determine nutritional status of the children. The DHS Program uses standardized procedures to collect anthropometric data across countries thereby ensuring comparability (Allen et al., 2019; Assaf et al., 2015; The DHS Program, 2020). In the DHS survey, children aged 6–59 months with haemoglobin (Hb) levels less than 11.0 g/dl were classified as anaemic (Croft et al., 2023).

2.5. Covariate assessment

Covariates adjusted for in the analysis were mother's education level, mother's age at the child's birth, household wealth status, type of residence (urban vs. rural), and household environmental quality (HEQ). Maternal education was classified into three levels: no formal education, primary education, and secondary education or higher education. Household wealth was determined by principal component analysis (PCA) of household assets with households classified into wealth tertiles (poor, middle and richest). The DHS Program uses PCA to construct the wealth index to ensure that asset-based disparities in countries were appropriately captured (Croft et al., 2023). HEQ was a latent trait variable generated from household sanitation (improved vs. unimproved), water sources (improved vs. unimproved), and household cooking fuel (clean vs. polluting) using item response theory with one-parameter logistic regression model that adjusts for complex survey design (Chen et al., 2021; Nguyen et al., 2022). Empirical Bayes means was used to predict the latent HEQ index and categorised into low, medium and high levels based on tertiles (Dwomoh et al., 2023).

2.6. Statistical analysis

We developed a hierarchical Bayesian spatial model to examine spatially varying effects of $PM_{2\cdot5}$ exposure on child health outcomes controlling for maternal, household and area-level covariates while explicitly accounting for the complex sampling design of the DHS. A Bayesian spatial multilevel mixed-effects model which allows for estimation of country-specific random effects was employed. This method allows for evaluation of variation in the outcome attributable to a country's distinct contextual factors (Aheto et al., 2021; Krainski et al., 2018).

Children served as the units of analysis at the lowest level of the hierarchy. The children are nested within EAs which in turn are nested within survey strata, sub-national levels and finally, countries. To capture unobserved heterogeneity across these levels, random intercepts were introduced for each level (Bakka et al., 2018). To account for the complex survey design and ensure the study findings are representative, all models were weighted using the DHS survey weights which were normalized at the country level.

A key feature of our model is the inclusion of a spatially varying random slope for $PM_{2\cdot5}$ exposure (Bakka et al., 2018; Bell et al., 2019). In modelling spatial autocorrelation, we first constructed a country-level adjacency matrix with neighbouring countries defined as those sharing a common border. This neighbourhood structure was then incorporated into the model's random effects through an intrinsic conditional autoregressive (ICAR) prior which allowed both the baseline risk (intercept) and the $PM_{2.5}$ effect (slope) to vary smoothly across adjacent countries. This allows the association between $PM_{2\cdot5}$ and child undernutrition to differ across countries thereby providing a more nuanced understanding of how local contextual factors modifies the effect of air pollution. To mitigate potential spatial confounding and improve model interpretability, the $PM_{2\cdot5}$ exposure variable was centred at the country level. For the main sub-regional analysis, exposure was centred at the country level whereas for the supplementary analysis (see Supplementary Material), centring was performed at the sub-national level.

2.7. Model specification

Let Y_{ijkl} denote the binary indicator of the health outcome for the i-th child in the j-th cluster (EA), within the k-th survey stratum and the l-th country. The probability of the outcome is $p_{ijkl} = Pr(Y_{ijkl} = 1)$, modeled as $Y_{ijkl} \sim Bernoulli(p_{ijkl})$. The linear predictor on the log-odds (logit) scale is:

$$logit(p_{ijkl}) = \eta_{ijkl}$$

We fitted two nested specifications under the Besag–York–Mollié 2 (BYM2) framework (Besag et al., 1991; Riebler et al., 2016) to account for both measured covariates and unmeasured spatial heterogeneity.

Model 1 (Exposure-only with spatially varying slope):

$$\eta_{ijkl} = \beta_0 + \beta_1\widetilde{x}_l + \beta_2\left(x_{ijkl} - \widetilde{x}_l\right) + \theta_l\left(x_{ijkl} - \widetilde{x}_l\right) + f(s_l + u_l) + \delta_k + \zeta_j$$

Model 2 (Fully adjusted with spatially varying slope):

$$\eta_{ijkl} = \beta_0 + \beta_1\widetilde{x}_l + \beta_2\left(x_{ijkl} - \widetilde{x}_l\right) + \beta_3\left(\mathscr{C}_{ijkl}\right) + \theta_l\left(x_{ijkl} - \widetilde{x}_l\right) + (s_l + u_l) + \delta_k + \zeta_j$$

Here, β_0 is the overall intercept. $\widetilde{x}_l$ is the country-level centred mean $PM_{2\cdot5}$ exposure. β_1 represents the average (fixed effect) association between the centred $PM_{2\cdot5}$ and the outcome across all countries. $\beta_2\left(x_{ijkl} - \widetilde{x}_l\right)$ represents the main fixed effect for the individual-level exposure centred at the country level. Both exposure variables were scaled by dividing by 10, so that the coefficients represent the effect of a 10 μg/m^3 change. $\mathscr{C}_{ijkl,,,}$ is a vector of child, maternal, and household-level covariates with a corresponding vector of fixed-effect coefficients β_3. The term $\theta_l\left(x_{ijkl} - \widetilde{x}_l\right)$ is the country-specific random slope for the centred $PM_{2\cdot5}$ exposure which allows the effect of individual exposure to vary by country l. This term is modelled with a spatially structured prior, $\theta_l \sim ICAR(\sigma_\theta^2)$, to capture spatial dependency in the exposure–response relationship. The term $f(s_l + u_l)$ is the country-level random intercept specified using the BYM2 framework. This partitions country-level heterogeneity into a spatially structured component s_l and an unstructured component u_l. The structured effect s=(s_1, …, s_l) follows an

intrinsic conditional autoregressive (ICAR) prior:

$$s_l|s_{-l} \sim \mathcal{N}\left(\frac{1}{n_l}\sum_{i\sim l} s_i, \sigma_s^2/n_l\right)$$

where the sum is taken over the n_l neighbors of country l. The unstructured spatial effect component is given as $u_l \sim \mathcal{N}(0, \sigma_u^2)$. Finally, δ_k and ζ_j are unstructured random intercepts for each country's region, the sample cluster (EA), and the survey stratum, respectively, with priors $\delta_k \sim \mathcal{N}(0, \sigma_\delta^2)$ and $\zeta_j \sim \mathcal{N}(0, \sigma_\zeta^2)$. These spatial terms are modelled as IID normal random variables.

We adopted a full Bayesian binomial regression framework estimating model parameters via Integrated Nested Laplace Approximation (INLA) as implemented in R-INLA (Lindgren and Rue, 2015; Rue et al., 2009). Country-level spatial dependence was accommodated through the BYM2 specification (Besag et al., 1991; Riebler et al., 2016) which merges spatially structured and unstructured random effects into a single, scaled component. In this reparameterization, the total precision parameter $\tau = {}^1/_{\sigma^2}$ regulates overall spatial variability while the mixing parameter $\phi \in [0, 1]$ determines the fraction of variance attributed to the structured (ICAR) component versus the unstructured effect (Morris et al., 2019). Weakly informative Penalized Complexity (PC) priors were specified for all random effect hyperparameters with the model relying on default vague Gaussian priors (N(0, 1000)) for the fixed effects. For the BYM2 spatial effect, the PC prior for the marginal standard deviation was specified as $P(\sigma > 1) = 0.01$ and the prior for the mixing parameter was $P(\phi < 0.5) = 0.5$. The country-level random slope for $PM_{2.5}$ exposure was modelled with a PC prior of $P(\sigma > 0.5) = 0.01$. The unstructured variability at the cluster and strata levels was modelled using IID random effects and also assigned PC prior of $P(\sigma > 1) = 0.01$. The PC priors were chosen following the recommendations of Simpson et al. (2017) to penalize complexity while retaining flexibility. We chose weakly informative thresholds to reflect plausible spatial and effect constraints which enables data-driven inference without imposing strong assumptions This is an appropriate strategy given limited prior knowledge on $PM_{2.5}$ effects in sub-Saharan Africa.

2.8. Sampling weight

The DHS household weights (variable v005) was rescaled and then normalized to match the analytic sample to ensure that the sum of the weights equalled the sample size thereby preserving the original sample size while also correcting for selection probabilities (Croft et al. 2023). The normalized weights were incorporated into the INLA model to ensure the parameter estimates reflected the population structure in the DHS sample. The approach adopted aligns with best practices for incorporating survey weights into Bayesian models (Chen et al., 2021; Si et al., 2020).

All analyses were conducted using the R-INLA framework (Lindgren and Rue, 2015; Rue et al., 2009) with statistical significance based on 95% Bayesian credible intervals (CrI). We produced interactive, web-based maps of the estimated spatial effects for effective policy-decision making. We predicted probabilities across all 34 SSA countries (see Supplementary Material). These visualizations were developed using the spdep, sp, and leaflet packages in R version 4.50 (Bivand et al., 2017; Cheng et al., 2019; RStudio Team, 2021). To visualize the spatial patterns and the certainty of the country-specific random slopes, we calculated and mapped the posterior exceedance probability defined as probability that the odds ratio for the $PM_{2.5}$ effect is greater than one (See Supplementary Material).

2.9. Ethical considerations

DHS surveys are conducted under the scientific and technical supervision of the Statistical and Health authorities in the respective countries. All the survey methods and procedures were carried out in accordance with relevant guidelines and regulations of the organisations in the countries. The survey protocols were approved by ICF International through The DHS Program and complies with U.S Department of Health and Human Services requirements (45 CFR 46). Informed consent was obtained from all subjects before the interview.

3. Results

Fig. 1 is a flowchart of the study sample selection process. A total of 855,395 children with complete exposure data (prenatal and postnatal) were included in the study.

Table 1 presents the distribution of study outcomes in the study population, and the regional variations. Of the total study sample, 16.9% were stunted, 9.2% were wasted, 4.2% were underweight, and 20.8% were anaemic. A substantial proportion of children had missing anthropometric data, 45.9% for stunting, 49% for wasting and underweight, and 67.9% for anaemia. West Africa recorded the highest proportion of stunted (46.8%), wasted (55.8%), underweight (63.1%), and

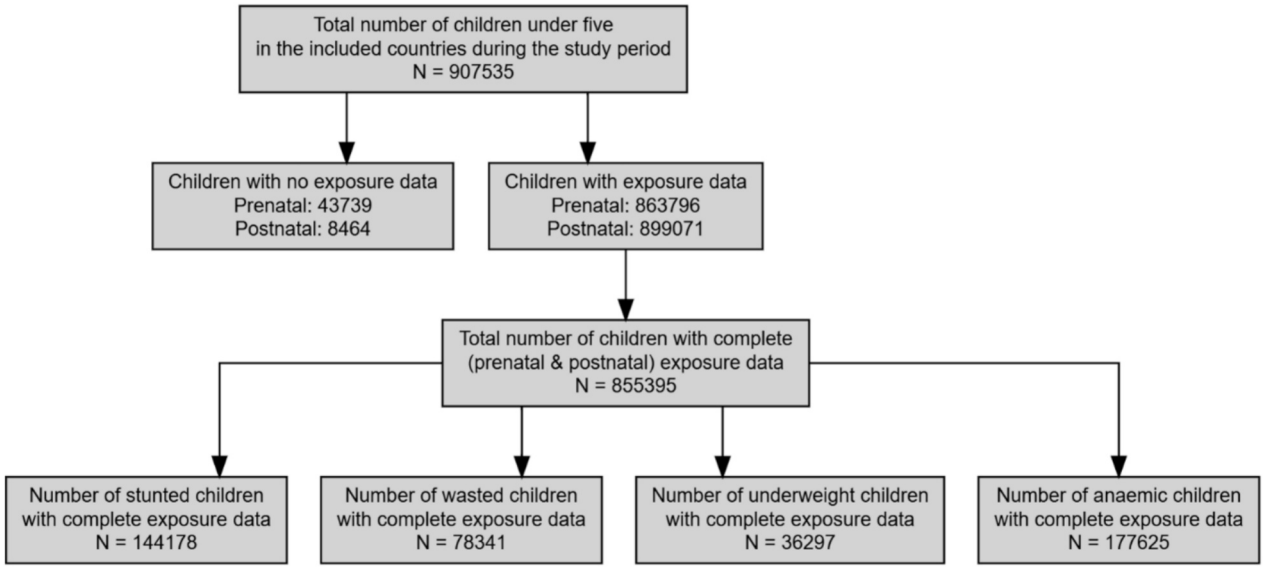

Fig. 1. Flowchart of study sample selection process.

Table 1
Distribution of the study outcomes in the study population (N = 855,395).

	Stunting N (%)	Wasting N (%)	Underweight N (%)	Anaemia N (%)
Outcome				
Yes	144,178 (16.9)	78,341 (9.2)	36,297 (4.2)	177,625 (20.8)
No	318,365 (37.2)	358,239 (41.9)	400,338 (46.8)	97,267 (11.4)
Missing	392,852 (45.9)	418,815 (49)	418,760 (49)	580,503 (67.9)
Sub-region				
West Africa	67,518 (46.8)	43,724 (55.8)	22,917 (63.1)	97,300 (54.8)
East Africa	57,919 (40.2)	24,613 (31.4)	9447 (26)	55,131 (31)
Central Africa	15,964 (11.1)	8745 (11.2)	3366 (9.3)	22,551 (12.7)
Southern Africa	2777 (1.9)	1259 (1.6)	567 (1.6)	2643 (1.5)

Table 2
Socio-demographic characteristics of undernourished children in the study sample.

Study Characteristics	Stunting N = 144,178 n (%)	Wasting N = 78,341 n (%)	Underweight N = 36,297 n (%)	Anaemia N = 177,625 n (%)
Gender				
Male	77,806 (54)	42,219 (53.9)	19,825 (54.6)	91,764 (51.7)
Female	66,372 (46)	36,122 (46.1)	16,472 (45.4)	85,861 (48.3)
Residence				
Urban	33,021 (22.9)	17,540 (22.4)	9807 (27)	48,698 (27.4)
Rural	111,157 (77.1)	60,801 (77.6)	26,490 (73)	128,927 (72.6)
Mothers' Age at time of survey				
<20 years	90,918 (63.1)	49,585 (63.3)	22,508 (62)	107,284 (60.4)
20–24 years	42,341 (29.4)	22,679 (28.9)	10,672 (29.4)	55,296 (31.1)
25–29 years	9510 (6.6)	5283 (6.7)	2678 (7.4)	12,993 (7.3)
>30 years	1409 (1)	794 (1)	439 (1.2)	2052 (1.2)
Mothers' Education Level				
No Education	69,086 (47.9)	44,603 (56.9)	21,093 (58.1)	86,424 (48.7)
Primary Education	50,625 (35.1)	22,508 (28.7)	8932 (24.6)	56,001 (31.5)
Secondary/Higher	24,458 (17)	11,228 (14.3)	6268 (17.3)	35,194 (19.8)
Missing	9	2	4	6
Wealth Status				
Poor	80,127 (55.6)	45,659 (58.3)	19,574 (53.9)	87,236 (49.1)
Middle	29,129 (20.2)	15,065 (19.2)	6895 (19)	35,280 (19.9)
Rich	34,921 (24.2)	17,616 (22.5)	9828 (27.1)	50,363 (28.4)
Missing	1	1		4746 (2.7)
HEQ				
Low	85,450 (59.3)	45,916 (58.6)	19,446 (53.6)	90,198 (50.8)
Medium	45,973 (31.9)	25,385 (32.4)	12,804 (35.3)	61,008 (34.3)
High	10,722 (7.4)	5978 (7.6)	3531 (9.7)	23,178 (13)
Missing	2033 (1.4)	1062 (1.4)	516 (1.4)	3241 (1.8)

anaemic (54.8%) children. Southern Africa recorded the lowest proportion of all the undernutrition outcomes; stunting (1.9%), wasting (1.6%), underweight (1.6%) and anaemia (1.5%).

The socio-demographic characteristics of the undernourished children in the study sample is presented in Table 2. Males had the highest proportion of undernourished children across all study outcomes; stunting (54%), wasting (53.9%), underweight (54.6%), and anaemia (51.7%). Children residing in rural areas recorded the highest proportion of undernourished children across all study outcomes; stunting (77.1%), wasting (77.6%), underweight (73%), and anaemia (72.6%). Mothers aged less than 20 years recorded the highest proportion of undernourished children across all study outcomes; stunting (63.1%), wasting (63.3%), underweight (62%), and anaemia (60.4%). Mothers with no formal education recorded the highest proportion of undernourished children; stunting (47.9%), wasting (56.9%), underweight (58.1%), and anaemia (48.7%). Poor households had the highest burden of undernourished children; stunting (55.6%), wasting (58.3%), underweight (53.9%), and anaemia (49.1%). Households with low HEQ had the highest burden of undernourished children; stunting (59.3%), wasting (58.6%), underweight (53.6%), and anaemia (50.8%).

Table 3 presents the average prenatal and postnatal $PM_{2.5}$ exposure levels among the undernourished children. Prenatal and postanal exposure levels was highest in West and Central Africa for all study outcomes. Paired t-tests revealed statistically significant differences between prenatal and postnatal $PM_{2.5}$ exposure for all undernutrition outcomes and regions ($p < 0.05$), with most comparisons showing highly significant differences ($p < 0.001$). Prenatal exposure was generally higher than postnatal exposure with the most pronounced differences observed in West Africa. $PM_{2.5}$ exposure levels among children who were not malnourished was similar across the undernutrition types (Supplementary Table S2).

Table 4 presents odds ratio and their corresponding 95% credible intervals (CrI) for the association between prenatal and postnatal $PM_{2.5}$ exposure and the child undernutrition outcomes. A 10 $\mu g/m^3$ increase in prenatal and postnatal $PM_{2.5}$ exposure was associated with 11% (AOR = 1.11; 95% CrI: 1.04, 1.20) and 9% (AOR = 1.09; 95% CrI: 1.04, 1.15) increased odds of stunting, respectively, in SSA. The increased odds of stunting for both prenatal and postnatal $PM_{2.5}$ exposure was highest in West Africa. Spatial variation in $PM_{2.5}$ exposure – stunting effects across SSA countries is presented in Fig. 2 with notable differences in the effect estimates observed across SSA countries. The observed spatial variation is confirmed by the spatial heterogeneity analysis results presented in Supplementary Table S4. The adjusted phi (φ) parameter which represents the proportion of variance attributed to structured spatial effects in the INLA BYM2 model was 0.75 (95% CrI: 0.30, 0.98) for postnatal exposure and 0.85 (95% CrI: 0.58, 0.99) for prenatal exposure in SSA. The heterogeneity was particularly pronounced in East Africa which recorded the highest adjusted φ of 0.53 and 0.54 for prenatal and postnatal exposure, respectively (Supplementary Table S7).

A 10 $\mu g/m^3$ increase in prenatal and postnatal $PM_{2.5}$ was associated with a 5% (AOR = 1.05; 95% CrI: 0.99, 1.10) and 6% (AOR = 1.06; 95% CrI: 1.02, 1.11) increased odds of wasting in SSA, respectively. The observed association between prenatal $PM_{2.5}$ and wasting were, however, not statistically significant. West Africa recorded the highest increased odds of wasting for both prenatal and postnatal $PM_{2.5}$ exposure. Spatial variation in $PM_{2.5}$ exposure – wasting effects across SSA countries is presented in Fig. 2 with notable differences in the effect estimates observed across SSA countries. The observed spatial variation is confirmed by the spatial heterogeneity analysis results presented in Supplementary Table S4. The adjusted φ for prenatal and postnatal exposure across SSA countries was 0.20 (95% CrI: 0.03, 0.73) and 0.24 (95% CrI: 0.01,0.85), respectively. The proportion of spatial heterogeneity varied with Central Africa recording the largest adjusted φ for both prenatal and postnatal exposure (Supplementary Table S6).

No association was found between prenatal and postnatal $PM_{2.5}$ exposure and underweight in SSA. In the sub-regional analysis, we

Table 3
Average prenatal and postnatal $PM_{2.5}$ exposure ($\mu g/m^3$) among undernourished children.

	Stunting Prenatal Mean (SD)	Postnatal Mean (SD)	p value	Wasting Prenatal Mean (SD)	Postnatal Mean (SD)	p value	Underweight Prenatal Mean (SD)	Postnatal Mean (SD)	p value	Anemia Prenatal Mean (SD)	Postnatal Mean (SD)	p value
All countries	35.7 (19)	35.1 (18.5)	<0.001	35.4 (18.8)	35.2 (18.4)	<0.001	35.5 (18.8)	35.2 (18.4)	<0.001	33.4 (15.3)	33.6 (14.9)	<0.001
West Africa	45.0 (20.4)	44.4 (19.7)	<0.001	44.5 (19.9)	43.9 (19.2)	0.001	44.5 (19.9)	43.9 (19.2)	<0.001	39.6 (15.5)	39.0 (14.8)	<0.001
East Africa	22.8 (8.3)	22.6 (8.2)	<0.001	23.1 (8.2)	22.3 (8.2)	<0.001	23.1 (8.2)	22.9 (8.2)	0.003	25.3 (9.8)	25.3 (9.9)	<0.001
Central Africa	38.6 (15.3)	38.8 (15.4)	0.043	38.6 (15.9)	38.8 (15.5)	0.001	38.6 (15.4)	38.8 (15.5)	<0.001	38.5 (16.3)	38.7 (16.3)	<0.001
Southern Africa	21.8 (7.7)	21.3 (7.4)	<0.001	21.8 (7.6)	21.3 (7.6)	<0.001	21.8 (7.6)	21.3 (7.3)	<0.001	25.2 (7.8)	24.2 (7.7)	<0.001

p values from paired t-tests comparing mean prenatal and postnatal $PM_{2.5}$ exposure within each undernutrition category.
SD: Standard Deviation

observed a positive association in Southern Africa for both prenatal and postnatal $PM_{2.5}$, and in West Africa for prenatal $PM_{2.5}$. The associations were, however, not statistically significant. Spatial variation in $PM_{2.5}$ exposure – underweight effects across SSA countries is presented in Fig. 2 with notable differences in the effect estimates across SSA countries. The observed spatial variation is confirmed by the spatial heterogeneity analysis results presented in Supplementary Table S4. The adjusted phi (φ) parameter for prenatal and postnatal exposure across SSA countries was 0.37 (95% CrI: 0.08, 0.63) and 0.42 (95% CrI: 0.12, 0.73), respectively. East Africa and Southern Africa recorded the highest regional φ values (Supplementary Table S7 and S8).

No association was found between prenatal and postnatal $PM_{2.5}$ exposure and anaemia in SSA. However, in Central Africa and Southern Africa, both prenatal and postnatal exposures was associated with decreased odds of anaemia. In Central Africa, the AORs were 0.85 (95% CrI: 0.72, 1.00) for prenatal and 0.87 (95% CrI: 0.80, 0.98) for postnatal exposure. In Southern Africa, the AORs were 0.76 (95% CrI: 0.59, 0.95) for prenatal and 0.79 (95% CrI: 0.61, 0.96) for postnatal exposure. Spatial variation in $PM_{2.5}$ exposure – anaemia effects across SSA countries is presented in Fig. 2 with notable differences in the effect estimates across SSA countries. The observed spatial variation is confirmed by the spatial heterogeneity analysis results presented in Supplementary Table S4. The adjusted phi (φ) parameter for prenatal exposure across SSA countries was very high (0.69; 95% CrI: 0.44, 0.94). For postnatal exposure, the adjusted φ was 0.64 (95% CrI: 0.24, 0.92). Central Africa and Southern Africa recorded the largest adjusted φ values (Supplementary Table S6 and S8). The country-specific effect estimates for all the studied outcomes are presented in Supplementary Table S9.

4. Discussion

This study represents the most comprehensive analysis to date on the association between ambient $PM_{2.5}$ exposure and child undernutrition in sub-Saharan Africa (SSA). We found prenatal and postnatal $PM_{2.5}$ exposure to be associated with child undernutrition in SSA. We observed spatial heterogeneity in the $PM_{2.5}$ exposure – child undernutrition effects between and within SSA countries.

4.1. Synthesis with previous evidence

Our results are consistent with a growing body of evidence implicating air pollution exposure with adverse child undernutrition outcomes. Prenatal and postnatal $PM_{2.5}$ exposure was associated with increased odds of stunting in SSA with the exposure – health effects found to be highest in West Africa. Our finding are consistent with the findings of other studies conducted on the continent (Amegbor et al., 2023; deSouza et al., 2022; Clarke et al., 2022) that also found prenatal $PM_{2.5}$ exposure to be associated with stunting. However, our estimates are very robust with consideration for both within- and between-area variation as against the fixed-effects models employed by deSouza et al. (2022). Fixed-effects models are conservative by design, relying only on within-unit variation and are highly susceptible to attenuation bias when exposure is measured with error (Bell and Jones, 2015; Wooldridge, 2010).

Postnatal $PM_{2.5}$ was associated with increased odds of wasting in SSA with West Africa recording the highest exposure – health effects. No association was observed between prenatal and postnatal $PM_{2.5}$ exposure and underweight in SSA. The distinct biological mechanisms for the two outcomes possibly explain the contrasting findings. Air pollution-induced stunting arises from chronic exposure (Sinharoy et al., 2020) whereas air pollution-induced acute malnutrition (wasting and underweight) may result indirectly from air pollution-induced respiratory infections (Yang et al., 2020). It is therefore possible that, air pollution was not very high enough to trigger respiratory illnesses and subsequently leading to wasting and underweight (Amir-ud-Din et al., 2024).

No association was found between prenatal and postnatal $PM_{2.5}$ exposure and anaemia in SSA. However, in Central Africa and Southern Africa, both prenatal and postnatal exposures was associated with decreased odds of anaemia. Our findings is contrary to the findings of Amegbor (2022) study which found a significant positive association. The contrasting findings could be explained by differences in the methodological approach by both studies. Amegbor (2022) study estimated a single pooled effect for the entire continent whereas our Bayesian spatial model incorporated a spatially varying random slope. This robust approach allows the magnitude of the $PM_{2.5}$ – anaemia association to differ by country thereby revealing significant geographic heterogeneity that a uniform effect model would otherwise mask.

The null findings in the anaemia analysis can also be attributed to other important determinants such as iron deficiency, malaria, and parasitic infections which are highly prevalent in SSA (Amegbor, 2022) and for which we had no data to control for their confounding effects.

4.2. Spatial heterogeneity

The geographic patterning of $PM_{2.5}$ effects reveals distinct spatial signatures across all the child undernutrition outcomes studied. Stunting demonstrates notable continental clustering; $\phi = 0.85$ and 0.75 for prenatal and postnatal exposure, respectively (Supplementary Table S4) and is a suggestion that impairment of chronic growth follows macro-regional environmental gradients like transboundary pollution and shared climate patterns. In contrast, wasting and underweight show minimal spatial structure with ϕ between 0.20 and 0.42 (Supplementary Table S4) and is a suggestion that these acute malnutrition outcomes respond primarily to localized household-level factors rather than regional $PM_{2.5}$ exposure. Anaemia presents an intermediate spatial profile ($\phi = 0.64$–0.69) and reflects hybrid regional environmental and local biological influences where $PM_{2.5}$ likely interacts with nutritional and parasitic determinants. (Ansah et al., 2024; Berg et al., 2024;

Table 4
Association between Prenatal and Postnatal $PM_{2.5}$ Exposure and Child Undernutrition in Sub-Saharan Africa.

Outcomes	Regions	Prenatal Exposure		Postnatal Exposure	
		Crude OR (95% CrI)	Adjusted OR (95% CrI)	Crude OR (95% CrI)	Adjusted OR (95% CrI)
Stunting	**All countries (n = 34)**	1.12 (1.03, 1.21)	1.11 (1.04, 1.20)	1.10 (1.04, 1.16)	1.09 (1.04, 1.15)
	West Africa (n = 14)	1.23 (1.16, 1.29)	1.20 (1.14, 1.27)	1.26 (1.19, 1.34)	1.22 (1.16, 1.29)
	East Africa (n = 12)	1.03 (0.91, 1.15)	1.04 (0.94, 1.16)	1.00 (0.92, 1.07)	1.02 (0.95, 1.08)
	Central Africa (n = 5)	1.07 (0.97, 1.20)	1.07 (0.98, 1.18)	0.97 (0.91, 1.05)	0.95 (0.93, 1.05)
	Southern Africa (n = 3)	0.94 (0.78, 1.16)	0.93 (0.77, 1.13)	0.95 (0.81, 1.14)	0.93 (0.80, 1.12)
Wasting	**All Countries (n = 34)**	1.05 (0.99, 1.11)	1.05 (0.99, 1.10)	1.07 (1.02, 1.13)	1.06 (1.02, 1.11)
	West Africa (n = 14)	1.17 (1.11, 1.23)	1.14 (1.09, 1.21)	1.19 (1.12, 1.26)	1.16 (1.10, 1.22)
	East Africa (n = 12)	0.95 (0.86, 1.00)	0.94 (0.88, 1.01)	1.01 (0.94, 1.08)	1.01 (0.95, 1.08)
	Central Africa (n = 5)	1.03 (0.93, 1.13)	1.03 (0.94, 1.12)	0.95 (0.89, 1.05)	0.96 (0.91, 1.03)
	Southern Africa (n = 3)	1.00 (0.84, 1.21)	1.02 (0.85, 1.23)	1.05 (0.86, 1.29)	1.05 (0.86, 1.29)
Underweight	**All Countries (n = 34)**	0.98 (0.92, 1.05)	0.98 (0.92, 1.04)	0.98 (0.90, 1.06)	0.95 (0.88, 1.03)
	West Africa (n = 14)	1.07 (0.99, 1.15)	1.06 (0.99, 1.13)	0.96 (0.88, 1.05)	0.95 (0.87, 1.03)
	East Africa (n = 12)	0.89 (0.79, 0.99)	0.90 (0.80, 1.00)	0.94 (0.83, 1.07)	0.95 (0.84, 1.08)
	Central Africa (n = 5)	0.97 (0.87, 1.07)	0.97 (0.87, 1.07)	0.98 (0.90, 1.08)	0.98 (0.89, 1.08)
	Southern Africa (n = 3)	1.02 (0.79, 1.29)	1.05 (0.82, 1.33)	1.09 (0.87, 1.37)	1.10 (0.88, 1.38)
Anaemia	**All Countries (n = 33)**	0.96 (0.88, 1.05)	0.96 (0.89, 1.05)	0.97 (0.87, 1.08)	0.97 (0.87, 1.08)
	West Africa (n = 14)	1.05 (0.97, 1.12)	1.03 (0.96, 1.10)	1.04 (0.96, 1.13)	1.02 (0.94, 1.10)
	East Africa (n = 11)	1.02 (0.93, 1.12)	1.03 (0.94, 1.13)	1.03 (0.87, 1.22)	1.03 (0.88, 1.22)
	Central Africa (n = 5)	0.84 (0.71, 0.99)	0.85 (0.72, 1.00)	0.86 (0.79, 0.98)	0.87 (0.80, 0.98)
	Southern Africa (n = 4)	0.76 (0.59, 0.96)	0.76 (0.59, 0.95)	0.78 (0.61, 0.97)	0.79 (0.61, 0.96)

OR: Odds Ratio, CrI: Credible Interval.
Model adjusted for mother's age at birth, maternal residence (urban vs. rural), maternal educational level, household wealth status, and household environmental quality.

Strachan et al., 2023).

The study findings should, however, be interpreted with caution considering the methodological limitations of the modelling approach. The limited number of spatial units in the sub-regional analysis violates the fundamental requirements for reliable ϕ estimation resulting in unreliable statistical estimates as depicted by the wide width of the credible intervals which exceeds 0.50 (Riebler et al., 2016; Shi et al., 2019; Sommet and Morselli, 2017). In light of this, while the continental stunting patterns suggest meaningful spatial signals, the sub-regional estimates do not.

Notwithstanding these limitations, the observed spatial patterns align with the mechanistic understanding of undernutrition. The wide geographic distribution of stunting across sub-Saharan Africa is a reflection of its chronic nature for which the role of long-term exposure to environmental stressors such as $PM_{2.5}$ exposure cannot be downplayed and is supported by the hypothesis that air pollution is a persistent physiological stressor that impairs linear growth over time (Pun et al., 2021; Sinharoy et al., 2020). In contrast, the observed lack of association of $PM_{2.5}$ with underweight and anaemia likely reflects its acute and multifactorial etiology. Underweight is a composite indicator that is influenced by transient factors such as food insecurity and illness (Atalell et al., 2022; Khezri et al., 2025). The determinants of anaemia include nutritional deficits, genetic predispositions, and endemic parasitic infections which may overshadow the effects of air pollution (Chaparro and Suchdev, 2019).

4.3. Regional differences in $PM_{2.5}$ composition and sources

A key finding of this study is the significant regional variation in the association between $PM_{2.5}$ and child undernutrition with the risk being more pronounced in West Africa. This marked difference likely reflects a synergy between regionally distinct pollution profiles and underlying health burden which underscores the principle that $PM_{2.5}$ is not a uniform pollutant (Liang et al., 2022). The toxicity of particulate matter is intrinsically linked to its chemical composition which is determined by its source. In West Africa, a major contributor to $PM_{2.5}$ mass is windblown mineral dust from the Sahara Desert which is transported by Harmattan winds whereas in other sub-regions, the pollution mixture is influenced heavily by residential biomass burning (De Longueville et al., 2013; Doumbia et al., 2023; Health Effects Institute, 2022).This heterogeneity is critical because a microgram of $PM_{2.5}$ from desert dust does not exert the same biological effect as a microgram from industrial or biomass combustion sources (Alves et al., 2023; Jia et al., 2017). The specific chemical signature of pollutants dictates their health impact. Mineral dust for instance can be rich in transition metals and silica which are potent inducers of oxidative stress and pulmonary inflammation (He et al., 2019; Jomova and Valko, 2011). This suggests that the excess risk for stunting and wasting observed in West Africa may be attributable to the specific toxic properties of Saharan dust. Epidemiological evidence has linked Saharan dust exposure to adverse health outcomes including an increased incidence of respiratory symptoms in children which can indirectly compromise nutritional status by suppressing appetite and increasing susceptibility to infection (McElroy et al., 2022).

4.4. Validity of results

The present study is the most comprehensive and large-scale investigation to date in SSA on the exposure–response relationship between ambient $PM_{2.5}$ and child undernutrition. DHS surveys are nationally representative surveys with very large sample size and assures generalizability of the study findings. However, the high proportion of children with no anthropometric data and excluded from the study as a result has implications for external validity of the study findings.

The study deployed a fully Bayesian spatial framework that integrates the Besag–York–Mollié 2 (BYM2) model within the Integrated

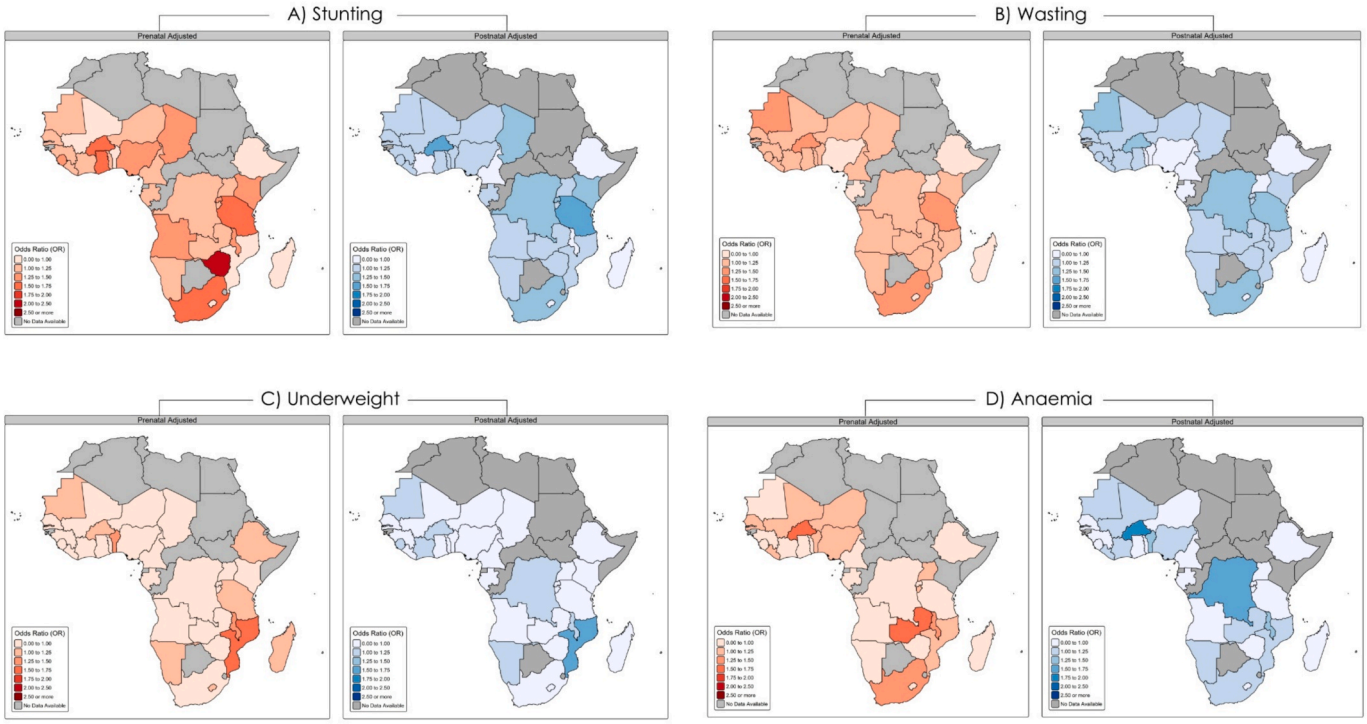

Fig. 2. Spatial Variation in the Association between $PM_{2.5}$ Exposure and Child Undernutrition Outcomes in Sub-Saharan Africa. (A) Stunting, (B) Wasting, (C) Underweight, and (D) Anaemia.

Nested Laplace Approximation (INLA) framework to help account for spatial autocorrelation and better investigate the spatially varying effects. A spatially random slope was introduced into the model to allow the $PM_{2.5}$ and child undernutrition relationship to vary across countries, and enabled formal quantification and mapping of spatial heterogeneity of the effect estimates. The BYM2 model compatibility with INLA permits efficient Bayesian inference and enables flexible specification of complex hierarchical relationships while leveraging default penalized complexity priors to guard against overfitting (Simpson et al., 2017). By embedding spatial smoothing within a multi-level mixed-effects framework, our approach yielded a more accurate localized estimates of air pollution effects on child undernutrition. In summary, our approach allowed us to quantify country- and regional-level effects whilst revealing how spatial dependence shapes the distribution of $PM_{2.5}$ – child undernutrition risk in SSA.

The study has some limitations which are worth pointing out. The cross-sectional design of DHS surveys means temporality cannot be established and threatens validity of the study findings. The reliance on satellite-derived ambient $PM_{2.5}$ concentrations is subject to measurement error with potential exposure misclassification. Prenatal $PM_{2.5}$ exposure assessment assumes that the study mothers stayed at the residential address at the time of the survey throughout the duration of pregnancy. This situation is likely not the case for some of the study mothers with potential exposure misclassification. In estimating prenatal exposure to $PM_{2.5}$, we assumed the duration of all pregnancies to be nine months with potential exposure misclassification. This is because DHS surveys do not collect information on the duration of pregnancy. We assigned 1998 monthly $PM_{2.5}$ averages to children born in early 1997 (i.e. up to three prenatal months in 1997) assuming minimal temporal variation across adjacent years. Exposure misclassification bias is also likely with this approach. However, considering the small group of children affected, the overall impact is likely minimal.

The DHS surveys rely on maternal self-report of sociodemographic and health history with potential for recall bias. Confounding bias is also likely in the study from the inability to adjust for important covariates such as malaria and other infections during pregnancy, pregnancy disorders (i.e. gestational diabetes, preeclampsia and other hypertensive disorders), pre-pregnancy BMI, nutritional status during pregnancy, alcohol intake during pregnancy, and passive and active smoking during pregnancy.

We checked for multicollinearity in our model by calculating the Variance Inflation Factors (VIF) for all the study outcomes using generalized linear model. We found all the VIF values to be below 5 which suggests no significant multicollinearity concerns in the study (Supplementary Table S3). Besides, we adjusted for the $PM_{2.5}$ exposure by subtracting the country average (i.e. centering of $PM_{2.5}$ exposure) which ensured that the individual-level exposure data where less related to the aggregate spatial effects. The centering of $PM_{2.5}$ exposure helped to avoid confusion among potentially correlated covariates whilst also addressing spatial confounding (Enders and Tofighi, 2007). Also, the weakly informative PC priors that we choose ensured regularization which enhanced numerical stability in the parameter estimation in the presence of correlated covariates.

5. Conclusions

We provide evidence of wide spatial heterogeneity in $PM_{2.5}$ effects on child undernutrition in SSA and underscores the need for geographical considerations in the development of interventions for addressing air pollution health effects. We have shown that deploying a *"one-size-fits-all"* approach for addressing air pollution effects on child health in SSA will not be effective and calls for region-specific strategies. To better inform these region-specific strategies, we have provided interactive web maps of country-specific and region-specific effect estimates (https://dice-aims1.github.io/AIM-1/) and we recommend that, they guide the work of children's environmental health practitioners in countries. The findings of this study will have profound implications for children's environmental health policy and practice in SSA.

CRediT author contribution statement.

Adeladza Kofi Amegah and Eric S. Coker designed the study, and together with Justice Moses K. Aheto and John Molitor guided Patrick Attey-Yeboah and Paul K. Adjorlolo to assemble the data and conduct

the data analysis. Patrick Attey-Yeboah wrote the manuscript with all authors reviewing drafts for important intellectual contributions.

CRediT authorship contribution statement

Patrick Attey-Yeboah: Writing – original draft, Methodology, Investigation, Formal analysis, Data curation. **Paul K. Adjorlolo:** Writing – review & editing, Methodology, Investigation, Formal analysis, Data curation. **Justice Moses K. Aheto:** Writing – review & editing, Methodology, Investigation. **John Molitor:** Writing – review & editing, Methodology, Investigation. **Eric S. Coker:** Writing – review & editing, Methodology, Investigation, Funding acquisition, Conceptualization. **Adeladza Kofi Amegah:** Writing – review & editing, Supervision, Project administration, Methodology, Investigation, Funding acquisition, Conceptualization.

Declaration of competing interest

The authors declare that they have no known competing financial interests or personal relationships that could have appeared to influence the work reported in this paper.

Acknowledgments

The study was funded by the National Institute Of Environmental Health Sciences of the National Institutes of Health, United States under Award Number U01ES036147. The content of this article is solely the responsibility of the authors and does not necessarily represent the official views of the National Institutes of Health, United States

Appendix A. Supplementary data

Supplementary data to this article can be found online at https://doi.org/10.1016/j.envint.2025.109995.

Data availability

Data will be made available on request.

References

Adekoya, A., Tyagi, S.K., Duru, C.N., Satia, I., Paudyal, V., Kurmi, O.P., 2022. Effects of household air pollution (HAP) on cardiovascular diseases in low-and middle-income countries (LMICs): a systematic review and meta-analysis. Int. J. Environ. Res. Public Health 19, 9298. https://doi.org/10.3390/ijerph19159298.

Aheto, J.M.K., Utuama, O.A., Dagne, G.A., 2021. Geospatial analysis, web-based mapping and determinants of prostate cancer incidence in Georgia counties: evidence from the 2012–2016 SEER data. BMC Cancer 21, 508. https://doi.org/10.1186/s12885-021-08254-0.

Allen, C.K., Croft, T.N., Pullum, T.W., Namaste, S.M.L., 2019. Evaluation of indicators to monitor quality of Anthropometry data during fieldwork, DHS Working Paper No. 162. ICF, Rockville, Maryland, USA.

Alves, C., Evtyugina, M., Vicente, E., Vicente, A., Rienda, I.C., de la Campa, A.S., Tomé, M., Duarte, I., 2023. PM2.5 chemical composition and health risks by inhalation near a chemical complex. J. Environ. Sci. 124, 860–874. https://doi.org/10.1016/j.jes.2022.02.013.

Amegah, A.K., 2020. Improving Child Survival in Sub-Saharan Africa: Key Environmental and Nutritional Interventions. Ann. Glob. Health 86, 73. https://doi.org/10.5334/aogh.2908.

Amegbor, P.M., 2022. Early-life environmental exposures and anaemia among children under age five in Sub-Saharan Africa: an insight from the Demographic & Health Surveys. Sci. Total Environ. 832, 154957. https://doi.org/10.1016/j.scitotenv.2022.154957.

Amegbor, P.M., Sabel, C.E., Mortensen, L.H., Mehta, A.J., Rosenberg, M.W., 2023. Early-life air pollution and green space exposures as determinants of stunting among children under age five in Sub-Saharan Africa. J. Eposure Sci. Environ. Epidemiol. https://doi.org/10.1038/s41370-023-00572-8.

Amir-ud-Din, R., Kumar, R., Naeem, N., Khan, M., 2024. Air pollution and under-5 child mortality: linking satellite and IPUMS-DHS data across 41 countries in South Asia and Sub-Saharan Africa. BMC Public Health 24, 2996. https://doi.org/10.1186/s12889-024-20476-y.

Ansah, E.W., Maneen, S., Ephraim, A., Ocloo, J.E.Y., Barnes, M.N., Botha, N.N., 2024. Politics–evidence conflict in national health policy making in Africa: a scoping review. Health Res. Policy Syst. 22, 47. https://doi.org/10.1186/s12961-024-01129-3.

Anselin, L., 2022. Spatial econometrics. Handb. Spat. Anal. Soc. Sci. 101–122.

Assaf, S., Kothari, M.T., Pullum, T., 2015. An Assessment of the Quality of DHS Anthropometric Data, 2005–2014, DHS Methodological Reports, No. 16. ICF International, Rockville, Maryland, USA.

Atalell, K.A., Alemu, T.G., Wubneh, C.A., 2022. Mapping underweight in children using data from the five Ethiopia Demographic and Health Survey data conducted between 2000 and 2019: a geospatial analysis using the Bayesian framework. Front. Nutr. 9. https://doi.org/10.3389/fnut.2022.988417.

Bakka, H., Rue, H., Fuglstad, G., Riebler, A., Bolin, D., Illian, J., Krainski, E., Simpson, D., Lindgren, F., 2018. Spatial modeling with R-INLA: a review. Wiley Interdiscip. Rev. Comput. Stat. 10, e1443.

Bell, A., Fairbrother, M., Jones, K., 2019. Fixed and random effects models: making an informed choice. Qual. Quant. 53, 1051–1074. https://doi.org/10.1007/s11135-018-0802-x.

Bell, A., Jones, K., 2015. Explaining fixed effects: Random effects modeling of time-series cross-sectional and panel data. Polit. Sci. Res. Methods 3, 133–153. https://doi.org/10.1017/PSRM.2014.7.

van den Berg, M., Flavel, J., Schram, A., Friel, S., Gesesew, H.A., Baum, F., 2024. Social, cultural and political conditions for advancing health equity: examples from eight country case studies (2011–2021). BMJ Glob. Health 9. https://doi.org/10.1136/bmjgh-2024-015694.

Besag, J., York, J., Mollié, A., 1991. Bayesian image restoration, with two applications in spatial statistics. Ann. Inst. Stat. Math. 43, 1–20. https://doi.org/10.1007/BF00116466.

Bhutta, Z.A., Berkley, J.A., Bandsma, R.H., Kerac, M., Trehan, I., Briend, A., 2017. Severe childhood malnutrition. Nat. Rev. Dis. Primer 3, 1–18. https://doi.org/10.1038/nrdp.2017.67.

Bivand, R., Altman, M., Anselin, L., Assunção, R., Berke, O., Bernat, A., Blanchet, G., 2017. Package 'spdep. Spat. Depend. Weight. Schemes Stat. R Package Version 1.

Bora, K., 2021. Air Pollution as a Determinant of Undernutrition Prevalence among Under-five Children in India: an Exploratory Study. J. Trop. Pediatr. 67, 1–9. https://doi.org/10.1093/tropej/fmab089.

Burgert, C.R., Colston, J., Roy, T., Zachary, B., 2013. Geographic Displacement Procedure and Georeferenced Data Release Policy for the Demographic and Health Surveys, DHS Spatial Analysis Reports, No. 7. ICF International, Calverton, Maryland, USA.

Chaparro, C.M., Suchdev, P.S., 2019. Anemia epidemiology, pathophysiology, and etiology in low- and middle-income countries. Ann. N. Y. Acad. Sci. 1450, 15–31. https://doi.org/10.1111/nyas.14092.

Chen, Y., Li, X., Liu, J., Ying, Z., 2021. Item Response Theory – a Statistical Framework for. Educ. Psychol. Meas. 10.48550/arXiv, 2108.08604.

Cheng, J., Karambelkar, B., Xie, Y., Wickham, H., Russell, K., Johnson, K., Schloerke, B., Agafonkin, V., 2019. Package 'leaflet. R Package Version 2, 1.

Clarke, K., Rivas, A.C., Milletich, S., Sabo-Attwood, T., Coker, E.S., 2022. Prenatal Exposure to Ambient PM2.5 and Early Childhood Growth Impairment Risk in East Africa. Toxics 10, 705. https://doi.org/10.3390/toxics10110705.

Croft, T.N., Allen, C.K., Zachary, B.W., 2023. Guide to DHS Statistics. ICF.

De Longueville, F., Hountondji, Y.-C., Ozer, P., Marticorena, B., Chatenet, B., Henry, S., 2013. Saharan Dust Impacts on Air Quality: what are the potential Health risks in West Africa? Hum. Ecol. Risk Assess. Int. J. 19, 1595–1617. https://doi.org/10.1080/10807039.2012.716684.

Deng, Y., Steenland, K., Sinharoy, S.S., Peel, J.L., Ye, W., Pillarisetti, A., Eick, S.M., Chang, H.H., Wang, J., Chen, Y., Young, B.N., Clark, M.L., Barr, D.B., Clasen, on behalf of the H.I., Thomas F., 2024. Association of household air pollution exposure and anemia among pregnant women: Analysis of baseline data from 'Household Air Pollution intervention Network (HAPIN)' trial. Environ. Int. 190, 108815. https://doi.org/10.1016/j.envint.2024.108815.

deSouza, P.N., Hammer, M., Anthamatten, P., Kinney, P.L., Kim, R., Subramanian, S.V., Bell, M.L., Mwenda, K.M., 2022. Impact of air pollution on stunting among children in Africa. Environ. Health Glob. Access Sci. Source 21, 1–13. https://doi.org/10.1186/s12940-022-00943-y.

Doumbia, T., Liousse, C., Ouafo-Leumbe, M.-R., Ndiaye, S.A., Gardrat, E., Galy-Lacaux, C., Zouiten, C., Yoboué, V., Granier, C., 2023. Source Apportionment of Ambient Particulate Matter (PM) in two Western African Urban Sites (Dakar in Senegal and Bamako in Mali). Atmos. 14, 684. https://doi.org/10.3390/atmos14040684.

Dwomoh, D., Sewor, C., Annim, S.K., Stranges, S., Kandala, N.B., Amegah, A.K., 2023. Do dietary practices and household environmental quality mediate socio-economic inequalities in child undernutrition risk in West Africa? Public Health Nutr. 26, 1022–1033. https://doi.org/10.1017/S1368980022002269.

Enders, C.K., Tofighi, D., 2007. Centering predictor variables in cross-sectional multilevel models: a new look at an old issue. Psychol. Methods 12, 121–138. https://doi.org/10.1037/1082-989X.12.2.121.

Ferreira, H. da S., Junior, A.F.S.X., Assunção, M.L., Uchôa, T.C.C., Lira-Neto, A.B., Nakano, R.P., 2018. Developmental origins of health and disease: a new approach for the identification of adults who suffered undernutrition in early life. Diabetes Metab. Syndr. Obes. 11, 543–551. 10.2147/DMSO.S177486.

Ghosh, S., Chowdhury, S.D., Chandra, A.M., Ghosh, T., 2015. Grades of undernutrition and socioeconomic status influence cognitive development in school children of Kolkata. Am. J. Phys. Anthropol. 156, 274–285. https://doi.org/10.1002/ajpa.22648.

Grey, K., Gonzales, G.B., Abera, M., Lelijveld, N., Thompson, D., Berhane, M., Abdissa, A., Girma, T., Kerac, M., 2021. Severe malnutrition or famine exposure in childhood and cardiometabolic non-communicable disease later in life: a systematic

review. BMJ Glob. Health 6, e003161. https://doi.org/10.1136/bmjgh-2020-003161.
Hammer, M.S., van Donkelaar, A., Bindle, L., Sayer, A.M., Lee, J., Hsu, N.C., Levy, R.C., Sawyer, V., Garay, M.J., Kalashnikova, O.V., Kahn, R.A., Lyapustin, A., Martin, R.V., 2023. Assessment of the impact of discontinuity in satellite instruments and retrievals on global PM2.5 estimates. Remote Sens. Environ. 294, 113624. https://doi.org/10.1016/j.rse.2023.113624.
Hammer, M.S., van Donkelaar, A., Li, C., Lyapustin, A., Sayer, A.M., Hsu, N.C., Levy, R. C., Garay, M.J., Kalashnikova, O.V., Kahn, R.A., 2020. Global estimates and long-term trends of fine particulate matter concentrations (1998–2018). Environ. Sci. Technol. 54, 7879–7890. https://doi.org/10.1021/acs.est.0c01764.
Harttgen, K., Klasen, S., Vollmer, S., 2013. Economic Growth and Child Undernutrition in sub-Saharan Africa. Popul. Dev. Rev. 39, 397–412. https://doi.org/10.1111/j.1728-4457.2013.00609.x.
He, M., Ichinose, T., Yoshida, S., Nishikawa, M., Sun, G., Shibamoto, T., 2019. Role of iron and oxidative stress in the exacerbation of allergic inflammation in murine lungs caused by urban particulate matter <2.5 μm and desert dust. J. Appl. Toxicol. 39, 855–867. https://doi.org/10.1002/jat.3773.
Health Effects Institute, 2022. The State of Air Quality and Health Impacts in Africa. Boston, MA.
Jia, Y.-Y., Wang, Q., Liu, T., 2017. Toxicity Research of PM2.5 Compositions In Vitro. Int. J. Environ. Res. Public Health 14, 232. https://doi.org/10.3390/ijerph14030232.
Jomova, K., Valko, M., 2011. Advances in metal-induced oxidative stress and human disease. Toxicology 283, 65–87. https://doi.org/10.1016/j.tox.2011.03.001.
Khezri, R., Jahanian, S., Gholami, M., Rezaei, F., 2025. The global air pollution and undernutrition among children under five. Sci. Rep. 15, 2935. https://doi.org/10.1038/s41598-025-87217-y.
Kirolos, A., Goyheneix, M., Eliasz, M.K., Chisala, M., Lissauer, S., Gladstone, M., Kerac, M., 2022. Neurodevelopmental, cognitive, behavioural and mental health impairments following childhood malnutrition: a systematic review. BMJ Glob. Health 7, e009330. https://doi.org/10.1136/bmjgh-2022-009330.
Krainski, E., Gómez-Rubio, V., Bakka, H., Lenzi, A., Castro-Camilo, D., Simpson, D., Lindgren, F., Rue, H., 2018. Advanced spatial modeling with stochastic partial differential equations using R and INLA. Chapman and Hall/CRC.
Liang, R., Chen, R., Yin, P., van Donkelaar, A., Martin, R.V., Burnett, R., Cohen, A.J., Brauer, M., Liu, C., Wang, W., Lei, J., Wang, L., Wang, L., Zhang, M., Kan, H., Zhou, M., 2022. Associations of long-term exposure to fine particulate matter and its constituents with cardiovascular mortality: a prospective cohort study in China. Environ. Int. 162, 107156. https://doi.org/10.1016/j.envint.2022.107156.
Lindgren, F., Rue, H., 2015. Bayesian spatial modelling with R-INLA. J. Stat. Softw. 63, 1–25. https://doi.org/10.18637/jss.v063.i19.
McElroy, S., Dimitrova, A., Evan, A., Benmarhnia, T., 2022. Saharan Dust and Childhood respiratory Symptoms in Benin. Int. J. Environ. Res. Public Health 19, 4743. https://doi.org/10.3390/ijerph19084743.
Morales, F., Montserrat-De la Paz, S., Leon, M.J., Rivero-Pino, F., 2023. Effects of malnutrition on the immune system and infection and the role of nutritional strategies regarding improvements in children's health status: a literature review. Nutrients 16, 1. https://doi.org/10.3390/nu16010001.
Morris, M., Wheeler-Martin, K., Simpson, D., Mooney, S.J., Gelman, A., DiMaggio, C., 2019. Bayesian hierarchical spatial models: Implementing the Besag York Mollié model in stan. Spat. Spatio-Temporal Epidemiol. 31, 100301. https://doi.org/10.1016/j.sste.2019.100301.
Nguyen, T.H., Lee, C.S., Kim, M.T., 2022. Using item response theory to develop and refine patient-reported outcome measures. Eur. J. Cardiovasc. Nurs. 21, 509–515. https://doi.org/10.1093/eurjcn/zvac020.
Pickett, K.E., Pearl, M., 2001. Multilevel analyses of neighbourhood socioeconomic context and health outcomes: a critical review. J. Epidemiol. Community Health 55, 111–122. https://doi.org/10.1136/jech.55.2.111.
Pun, V.C., Dowling, R., Mehta, S., 2021. Ambient and household air pollution on early-life determinants of stunting—a systematic review and meta-analysis. Environ. Sci. Pollut. Res. 28, 26404–26412. https://doi.org/10.1007/s11356-021-13719-7.
Riebler, A., Sørbye, S.H., Simpson, D., Rue, H., 2016. An intuitive Bayesian spatial model for disease mapping that accounts for scaling. Stat. Methods Med. Res. 25, 1145–1165. https://doi.org/10.1177/0962280216660421.
RStudio Team, 2021. RStudio: Integrated development for R (manual). RStudio, PBC, Boston, MA.
Rue, H., Martino, S., Chopin, N., 2009. Approximate Bayesian inference for latent Gaussian models by using integrated nested Laplace approximations. J. R. Stat. Soc. Ser. B Stat. Methodol. 71, 319–392. https://doi.org/10.1111/j.1467-9868.2008.00700.x.
Shen, S., Li, C., van Donkelaar, A., Jacobs, N., Wang, C., Martin, R.V., 2024. Enhancing Global Estimation of Fine Particulate Matter Concentrations by Including Geophysical a Priori Information in Deep Learning. ACS EST Air 1, 332–345. https://doi.org/10.1021/acsestair.3c00054.
Shi, D., Lee, T., Maydeu-Olivares, A., 2019. Understanding the Model size effect on SEM Fit Indices. Educ. Psychol. Meas. 79, 310–334. https://doi.org/10.1177/0013164418783530.
Si, Y., Trangucci, R., Gabry, J.S., Gelman, A., 2020. Bayesian Hierarchical Weighting Adjustment and Survey Inference. 10.48550/arXiv, 1707.08220.
Simpson, D., Rue, H., Riebler, A., Martins, T.G., Sørbye, S.H., 2017. Penalising Model Component Complexity: a Principled, Practical Approach to Constructing Priors. Stat. Sci. 32, 1–28.
Sinharoy, S.S., Clasen, T., Martorell, R., 2020. Air pollution and stunting: a missing link? Lancet Glob. Health 8, e472–e475. https://doi.org/10.1016/S2214-109X(20)30063-2.
Sommet, N., Morselli, D., 2017. Keep calm and learn multilevel logistic modeling: a simplified three-step procedure using Stata, R, Mplus, and SPSS. Int. Rev. Soc. Psychol. 30, 203–218.
Strachan, D.L., Teague, K., Asefa, A., Annear, P.L., Ghaffar, A., Shroff, Z.C., McPake, B., 2023. Using health policy and systems research to influence national health policies: lessons from Mexico. Cambodia and Ghana. Health Policy Plan. 38, 3–14. https://doi.org/10.1093/heapol/czac083.
The DHS Program, 2020. The DHS Program. Collect. Qual. Anthr. Data DHS Program. URL https://blog.dhsprogram.com/collecting-quality-anthropometric-data-in-the-dhs-program/ (accessed 11.4.25).
UNICEF, WHO, & World Bank Group, 2023. Levels and trends in child malnutrition: UNICEF / WHO / world bank group joint child malnutrition estimates: Key findings of the 2023 edition (Joint Child Malnutrition Estimates). World Health Organization, https://www.who.int/publications/i/item/9789240073791.
van Donkelaar, A., Hammer, M.S., Bindle, L., Brauer, M., Brook, J.R., Garay, M.J., Hsu, N.C., Kalashnikova, O.V., Kahn, R.A., Lee, C., Levy, R.C., Lyapustin, A., Sayer, A.M., Martin, R.V., 2021. Monthly Global estimates of Fine Particulate Matter and their uncertainty. Environ. Sci. Technol. 55, 15287–15300. https://doi.org/10.1021/acs.est.1c05309.
Van Donkelaar, A., Martin, R.V., Brauer, M., Hsu, N.C., Kahn, R.A., Levy, R.C., Lyapustin, A., Sayer, A.M., Winker, D.M., 2016. Global estimates of fine particulate matter using a combined geophysical-statistical method with information from satellites, models, and monitors. Environ. Sci. Technol. 50, 3762–3772. https://doi.org/10.1021/acs.est.5b05833.
Vassilakou, T., 2021. Childhood Malnutrition: Time for Action. Children 8, 103. https://doi.org/10.3390/children8020103.
Victora, C.G., Adair, L., Fall, C., Hallal, P.C., Martorell, R., Richter, L., Sachdev, H.S., 2008. Maternal and child undernutrition: consequences for adult health and human capital. Lancet 371, 340–357. https://doi.org/10.1016/S0140-6736(07)61692-4.
Wooldridge, J.M., 2010. Econometric analysis of cross section and panel data, 2nd ed. MIT press.
Yang, L., Li, C., Tang, X., 2020. The Impact of PM2.5 on the Host Defense of respiratory System. Front. Cell Dev. Biol. 8. https://doi.org/10.3389/fcell.2020.00091.